Valence-band photoemission spectroscopy of the giant magnetoresistive spinel compound $Fe_{0.5}Cu_{0.5}Cr_2S_4$

J.-S. Kang,[1] Sam Jin Kim,[2] Chul Sung Kim,[2] C. G. Olson,[3] and B. I. Min[4]
[1]*Department of Physics, The Catholic University of Korea, Puchon 422-743, Korea*
[2]*Department of Physics, Kookmin University, Seoul 136-702, Korea*
[3]*Ames Laboratory, Iowa State University, Ames, Iowa 50011*
[4]*Department of Physics, Pohang University of Science and Technology, Pohang 790-784, Korea*
(Received 31 July 2000; revised manuscript received 20 November 2000; published 19 March 2001)

Electronic structures of the giant magnetoresistive $Fe_{0.5}Cu_{0.5}Cr_2S_4$ (FCCS) spinel compound have been investigated using photoemission spectroscopy (PES). Resonant PES measurements around the Cu, Fe, Cr $3p \rightarrow 3d$ absorption edges exhibit negligible resonant interference behavior for the Cu $3d$ valence electrons, indicating the monovalent valence state of the Cu ion in FCCS. The top of the valence band is found to be predominantly of the Cr $3d$ and the nearly filled Cu $3d$ electron character, whereas the Fe $3d$ electron character is distributed over the whole valence band. The measured valence-band PES spectra of FCCS yield better agreement with the LSDA$+U$ calculation than with the local spin-density approximation (LSDA) calculation, suggesting the importance of the large Coulomb interactions U between d electrons. On the other hand, the low spectral intensity near E_F in the measured valence-band spectrum suggests an extra localization in FCCS, not explained by the large U alone.

DOI: 10.1103/PhysRevB.63.144412 PACS number(s): 71.30.+h, 79.60.−i, 75.70.Pa

I. INTRODUCTION

The discovery of the colossal magnetoresistance phenomenon in the perovskite Mn oxides of $R_{1-x}A_xMnO_3$ (RAMO; R=rare earth, A=divalent or tetravalent cation) has generated wide attention[1] due to a variety of interesting physical properties and their potential for technological applications. Very large negative magnetoresistance (MR) has also been observed in the Cr-based chalcogenide spinel compounds $Fe_{1-x}Cu_xCr_2S_4$ (x=0,0.5), both of which are ferrimagnetic semiconductors at T=0 K.[2] In the spinel structure, the Fe and Cu ions occupy the tetrahedral sites and the Cr ions occupy the octahedral sites, surrounded by four and six sulfur ions, respectively. The observed MR of $Fe_{0.5}Cu_{0.5}Cr_2S_4$ (FCCS) was ~7% at T_C~340 K (T_C=the magnetic transition temperature) under the external magnetic field of 6 T. This size of MR is as large as in giant magnetoresistance (GMR) metallic multilayers. Similarly as in the perovskite manganites, a metal-insulator (M-I) transition occurs simultaneously with the magnetic transition in the spinel compounds. The temperature dependence of the resistivity ρ (T) shows the semiconducting behavior for $T>T_C$ and then the metallic feature below T_C down to ~150 K. Upon further cooling below ~150 K, the semiconducting behavior is observed again.

It has been pointed out that the mechanisms of the M-I transition and the magnetic transition in the spinel compounds are different from those in the perovskite manganites.[2] In a divalent ion-doped RAMO system, Mn ions exist in the formally trivalent and tetravalent states. Then the Zener-type double exchange (DE) between spin-aligned Mn^{3+} ($t_{2g}^3e_g^1$) and Mn^{4+} (t_{2g}^3) ions through oxygen ions yields the metallic conductivity and ferromagnetism.[3] In the DE model, there should exist mixed-valent ions to maintain the correlation between magnetism and conductivity. Further, the strong electron-phonon interaction due to the Jahn-Teller effect at the Mn^{3+} ion is invoked to elucidate the M-I transition in RAMO systems.[4] In contrast, there seems to be no evidence for the DE mechanism in $FeCr_2S_4$ (Ref. 5) and no Jahn-Teller active ions.[2]

One of the important issues in the chalcogenide spinel compounds is the valence states of constituent elements. Indeed, the question on the valency of Cu in CuM_2X_4 (M=transition metal element; X=S, Se, Te) has been a long-standing problem. Goodenough[6] claimed the Cu ion to be divalent, while Lotgering *et al.*[7] claimed it to be monovalent. If the Cu ion is monovalent in spinels, the valence configurations of the Cr ion in $CuCr_2S_4$ are expected to be $Cu^+(Cr^{3+}Cr^{4+})S_4^{2-}$, yielding a formal mixed valence of +3.5. Then the ferromagnetic ground state of $CuCr_2S_4$ can be explained in terms of the DE interaction.

Various experiments give different results on the valence state of the Cu ion in spinels. Core-level x-ray photoemission spectroscopy (XPS),[8–11] x-ray emission spectroscopy,[9,11] and the Cu K-edge x-ray absorption spectroscopy (XAS)[12] measurements on the spinel compounds of CuM_2X_4 (M=V, Cr, Rh, Ir; X=S, Se) suggested that the Cu ions in the spinels are monovalent. However, NMR,[13] neutron diffraction,[14] and magnetic[15] studies suggest that experimental results could be interpreted with the divalent Cu ions. Therefore it is essential to determine the valence states of the Cu and Cr ions in spinel compounds to understand the underlying physics properly. The core-level XPS study on $FeCr_2S_4$ and FCCS (Ref. 16) shows that the Cr ions are in the trivalent states ($3d^3$) in both compounds, whereas the Cu ion in FCCS is likely to be in the monovalent state ($3d^{10}$). Note that core-level XPS is rather an indirect probe for the valence electronic structures because the XPS spectra are determined by the final state effects which reflect the response of the valence electrons to the core hole created in the photoionization process. On the other hand, valence-band

photoemission spectroscopy (PES) provides direct information on the valence-band electronic structures of solids.

The information of the valence-band electronic structures of spinel compounds is very important because they determine the transport and magnetic properties of solids. In the late 1960s the schematic electronic structures of the spinel compounds were suggested based on empirical models.[6,7] With the recent development in the theoretical electronic structure calculations, more realistic electronic structures of various chalcogenide spinel compounds have been reported by performing the first-principles band-structure calculations.[11,17,18] However, there has been no experimental confirmation for the proposed electronic structures of $Fe_2Cr_2S_4$ and $Fe_{0.5}Cu_{0.5}Cr_2S_4$ yet, even though there are valence-band PES studies on some Cu-based chalcogenide sulfides CuM_2S_4 (M=V, Rh, Ir).[9–11]

In this paper, we report a temperature-dependent valence-band PES study of $Fe_{0.5}Cu_{0.5}Cr_2S_4$. Resonant photoemission spectroscopy (RPES) measurements near the Fe, Cu, Cr $3p \rightarrow 3d$ absorption edges have been performed. By varying the photon energy $h\nu$, the different electron character in the valence band and the Cu valency have been identified. Experimental results are compared to the band-structure calculations performed in the local spin-density functional approximation (LSDA) and the LSDA+U method (U =Coulomb correlation interaction).

II. EXPERIMENTAL AND COMPUTATIONAL DETAILS

Synthesis of the FCCS sample was accomplished by the following direct-composition method. Fe powder of 99.999%, Cu powder of 99.999%, and Cr powder of 99.995% purity were reduced by hydrogen gas at 700 °C. A mixture of proper portions of these powders and the sulphur powder of 99.9999% purity was sealed into an evacuated quartz tube. These mixture was heated at 120 °C for 12 h, at 500 °C for 24 h, and 1000 °C for 96 h, and then cooled down slowly to room temperature at a rate of 10 °C/h. For the purpose of eliminating the possibility of oxidation from the quartz tube wall it was necessary to flow nitrogen gas at the above firing stages. In order to obtain a homogeneous material, it was necessary to grind the sample after the first firing and press the powder into a pellet before heating it for a second time to 1050 °C for 99 h. The x-ray powder diffraction pattern showed a clean single spinel phase without detectable secondary phases. Resistivity and magnetization measurements showed a very similar behavior as in Ref. 2.

PES experiments were carried out at the ERG/Seya, Ames-Montana State beamline at the Synchrotron Radiation Center (SRC). Samples were fractured and measured at T <15 K in vacuum with a base pressure better than 3×10^{-11} Torr. The total instrumental resolution [full width at half maximum (FWHM)] was about 150 meV at photon energy $h\nu$=22 eV and 250 meV at $h\nu$=120 eV. Samples were fractured several times, and different fractures gave essentially same results. All the spectra were normalized to the mesh current.

Electronic structures and the projected angular momentum density of states (PLDOS) of FCCS have been calculated by employing the self-consistent linearized muffin-tin-orbital (LMTO) band method within the LSDA. The von Barth–Hedin form of the exchange-correlation potential has been utilized. The PLDOS has also been calculated by using the LSDA+U method that incorporates the on-site Coulomb interaction U.[19] Both the LSDA and LSDA+U calculations yield the ferrimagnetic and insulating ground state for $Fe_{0.5}Cu_{0.5}Cr_2S_4$.[18]

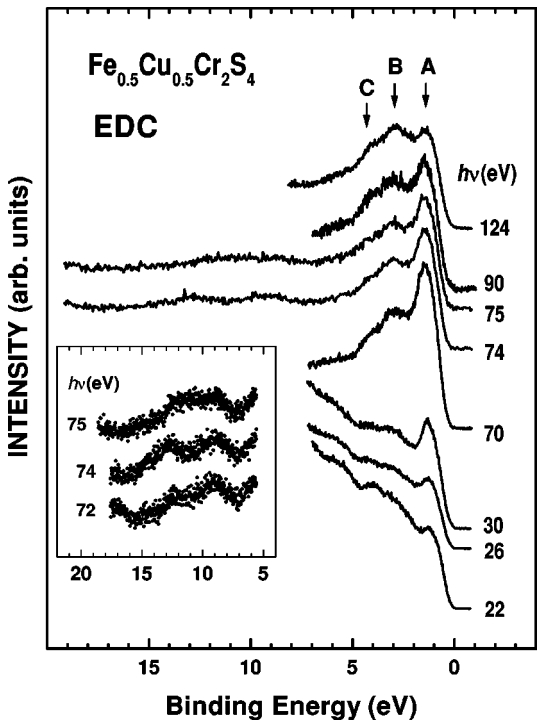

FIG. 1. Energy distribution curves (EDC's) of $Fe_{0.5}Cu_{0.5}Cr_2S_4$ (FCCS) over a photon energy ($h\nu$) range of 22 eV $\leqslant h\nu \leqslant$ 124 eV. Inset: details of the valence-band features in the Cu $3p \rightarrow 3d$ RPES region.

III. RESULTS AND DISCUSSION

Figure 1 presents the valence-band spectra of FCCS for 22 eV $\leqslant h\nu \leqslant$ 124 eV. The different line shapes with changing $h\nu$ are mainly due to the different relative strengths of the photoionization cross sections of different electronic states with $h\nu$. In the $h\nu$ range in this figure, the Fe $3d$, Cu $3d$, Cr $3d$, and S $3p$ emissions are comparable to one another. According to the atomic photoionization cross section,[20] the cross section ratios of Fe $3d$: Cu $3d$: Cr $3d$: S $3p$ in FCCS are about 11% : 14% : 62% : 13% at $h\nu \sim 26$ eV, about 17% : 24% : 44% : 15% at $h\nu \sim 80$ eV, and about 17% : 30% : 36% : 18% at $h\nu \sim 130$ eV. Due to the high inelastic backgrounds at low $h\nu$'s (22−30 eV), it is difficult to compare the relative peak intensities qualitatively at low $h\nu$'s, and so here we confine our discussion for $h\nu \geqslant 70$ eV. The feature A (−1.5 eV) decreases as $h\nu$ increases from 70 eV to 124 eV, suggesting that this peak has the significantly large Cr $3d$ character. This assignment is consistent with the CIS measurement (Fig. 2) and the theoretical calculations (Fig. 4). Relative to the intensity of the peak A,

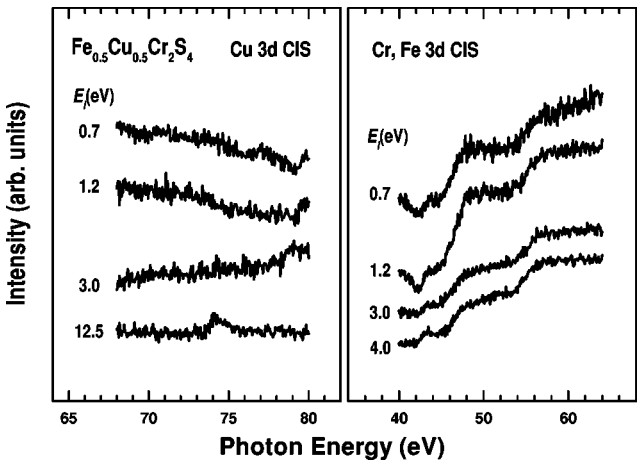

FIG. 2. Constant-initial-state (CIS) spectra of FCCS for several initial-state binding energies E_i, taken near the Cu $3p$ absorption threshold (left) and the Cr and Fe $3p$ absorption thresholds (right), respectively.

the high-binding-energy (BE) peak of C (-4.5 eV) increases slightly from 70 eV to 124 eV, suggesting the S $3p$ nature of this peak. The intermediate BE peak of B (-3 eV) seems to be mixed with the Fe $3d$, Cu $3d$, and S $3p$ electrons.[21] No metallic Fermi edge is observed in FCCS at $T\sim 15$ K, which is consistent with its insulating behavior at low T.

The inset of Fig. 1 shows the enlarged spectra for the region between 6 eV BE and 18 eV BE, where the Cu $3d^9 \rightarrow 3d^8$ satellite structures are expected if they exist. In many copper oxides, the Cu $3d$ satellite features have been observed around 12 eV BE,[22] signaling the large $3d$ Coulomb correlation interaction. A weak feature around 9 eV BE in FCCS is probably due to the emission from impurities in the grain boundaries of polycrystalline samples. Another weak feature at 13 eV BE at $h\nu=72$ eV reveals a weak enhancement around $h\nu=74$ eV, suggesting that this peak might be identified as the Cu $3d^9\rightarrow 3d^8$ satellite. The nature of this 13 eV peak will be further discussed in Fig. 2.

RPES for the Cu $3p$ absorption edge indicates that the Cu ions are nearly monovalent in FCCS, as explained below. RPES for the Cu $3p$ absorption edge involves atomic processes of the type

$$3p^6 3d^n + h\nu \rightarrow 3p^5 3d^{n+1} \rightarrow 3p^6 3d^{n-1}\epsilon_k, \qquad (1)$$

where ϵ_k denotes the emitted electron. The first step is a photoabsorption of a $3p$ electron to an unoccupied $3d$ state, leading to an intermediate state. The second step is a two-electron Coster-Kronig decay of the intermediate state, involving an Auger matrix element of the Coulomb interaction. The same final state can also be reached by a direct photoemission process

$$3p^6 3d^n + h\nu \rightarrow 3p^6 3d^{n-1}\epsilon_k. \qquad (2)$$

The interference between these two processes leads to the so-called Fano resonant or antiresonant line shape that depends on the details of the decay channels. For Cu, such a RPES process will not be invoked if Cu is monovalent (Cu^+: $3d^{10}$), whereas RPES proceeds for the divalent Cu ion (Cu^{2+}: $3d^9$).

The above argument of the monovalent Cu^+ ions in FCCS is supported by the constant-initial-state (CIS) spectra, shown in Fig. 2. In taking a CIS spectrum, $h\nu$ and E_K are simultaneously varied so as to maintain $E_i=h\nu-\phi-E_K$ to be constant (E_K=kinetic energy; ϕ=work function). Thus the CIS spectrum measures the relative strength of a given initial-state emission as a function of $h\nu$. The left panel of Fig. 2 shows the CIS spectra of FCCS for several initial-state binding energies E_i, taken in the Cu $3p\rightarrow 3d$ RPES region, and the right panel shows those in the Cr and Fe $3p\rightarrow 3d$ RPES regions. In these figures, the vertical scale is the same for all the curves.

The right panel of Fig. 2 shows the CIS spectra for 40 eV $\lesssim h\nu \lesssim$ 64 eV. The resonant features for 40 eV $\lesssim h\nu \lesssim$ 50 eV and for 50 eV $\lesssim h\nu \lesssim$ 60 eV are due to the Cr $3p\rightarrow 3d$ and Fe $3p\rightarrow 3d$ resonance, respectively. The larger resonant enhancement near the Cr $3p$ absorption edge than at the Fe $3p$ absorption edge reflects the larger number of the Cr ions per unit cell, compared to that of the Fe ions (4:1). Note that the Cr $3d$ electron character is concentrated predominantly near the top of the valence band, whereas the Fe $3d$ electron character is rather uniformly distributed over the whole valence band. This finding is consistent with that of Fig. 1 and the theoretical calculations in Fig. 4.

In contrast, the left panel shows that the main band emissions in the Cu $3p\rightarrow 3d$ CIS spectra exhibit no resonant enhancement nor antiresonant suppression that can be attributed to the Cu $3d$ electron character.[23] We interpret this result to reflect that the Cu $3d$ electrons in the main band have mainly the $3d^{10}$ character. On the other hand, the emission with $E_i=12.5$ eV shows a weak enhancement at around $h\nu=74$ eV, implying that this peak might be identified as the Cu $3d^9\rightarrow 3d^8$ satellite. However, the absence of the satellite structure in the Cu $2p$ XPS (Refs. 8 and 24) suggests that the weight of the Cu $3d^9$ configuration in the ground state is very small, even if it exists. Note that this enhancement is very weak compared to those of Fe and Cr $3d$ states, shown in the right panel of Fig. 2, or those of the formally divalent copper oxides, such as CuO (Ref. 23) and $La_{1.8}Sr_{0.2}CuO_4$ (Ref. 22). Due to its very weak intensity, it is difficult to tell whether this CIS spectrum has a Fano-type interference profile. Thus Fig. 2 indicates that the Cu $3p\rightarrow 3d$ RPES process is negligible in FCCS, indicating that the Cu ions are nearly monovalent or at least far from being divalent.

Figure 3 shows the temperature- (T-) dependent valence-band PES spectra of FCCS, obtained at $h\nu=70$ eV. The valence-band spectrum at 15 K (the semiconducting regime) is compared to the one at 150 K where the resistivity is minimum (the most metalliclike regime). Essentially no T-dependent changes occur in the large-energy-scale line shape. Further, no metallic Fermi edge is seen at the resistivity minimum (T=150 K), which is probably due to the still large resistivity of FCCS, $\rho(150\text{ K})\sim 0.25\ \Omega$ cm,[25] implying the very small metallic density of states (DOS) at E_F in FCCS. A high-resolution PES study on single-crystalline FCCS will help to resolve this problem. Figure 3 implies that

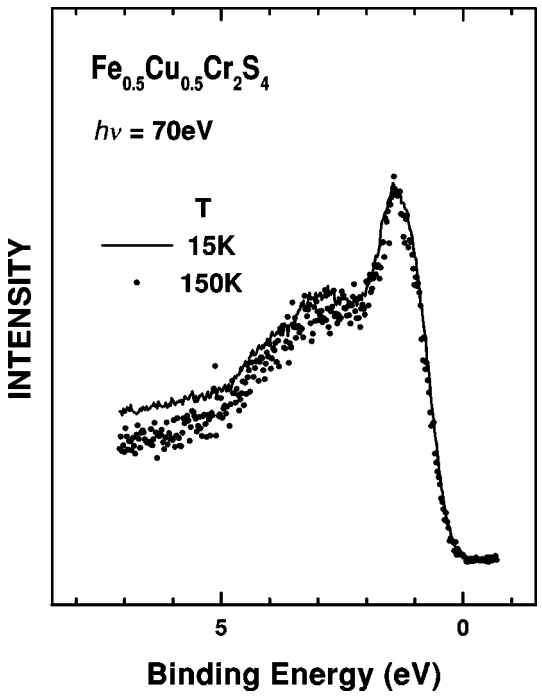

FIG. 3. Temperature-dependent valence-band spectra of FCCS with $h\nu = 70$ eV.

the character of the charge carriers does not change as the phase of FCCS changes from the semiconducting region to the metallic region.

Figure 4 shows the theoretical total DOS and PLDOS of FCCS, which are obtained from the LSDA calculations and by adding the spin-up and spin-down total DOS and PLDOS, respectively. The total DOS is per unit cell (two formula units) and each PLDOS is per atom. The ferrimagnetic and insulating ground state is revealed as a small gap at E_F in the total DOS. The valence band extends from E_F to approximately 7 eV below E_F, in agreement with the measured photoemission spectra (see Figs. 1 and 5). The Cu *d* bands are nearly filled, consistent with the finding of Figs. 1 and 2. The Fermi level lies near the top of the complex of the Cu *d*, Fe *d*, and Cr *d*, with the largest contribution from the Cu *d* electrons. The Fe and Cr *d* bands are much wider than the Cu *d* bands. The wide Fe *d* states below E_F correspond to the majority spin-down e_g and t_{2g} bands, and the unoccupied peaks above E_F correspond to the minority spin-down e_g and t_{2g} bands. Note that the Fe ions are located in the tetrahedral sites, and so the energy levels of e_g are lower than the energy levels of t_{2g}. The Cr *d* peaks below E_F correspond to the spin-up t_{2g} band, while the unfilled peaks above E_F correspond to the spin-up e_g and spin-down t_{2g} and e_g bands. Since the Cr ions are located in the octahedral sites, the situation is reversed from the case of Fe. Most of the S *p* states are located well below E_F with negligible DOS near E_F. The S *p* states overlap mainly with the Fe *d* states, but not with the Cu *d* states, indicating the large hybridization to the Fe *d* states, but a weak hybridization to the Cu *d* states. The relative positions of the Fe, Cu, Cr *d*, and S *p* bands in the LSDA+U calculations are similar to those in the LSDA calculations, and the above discussion holds for the LSDA +U case.[18]

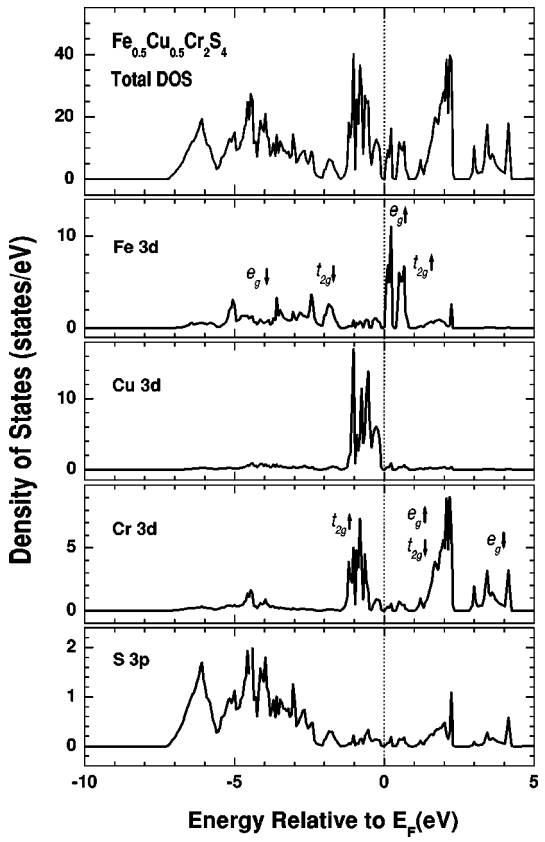

FIG. 4. Total and projected angular momentum density of states (PLDOS) from the LSDA calculations of FCCS. From top, total DOS per unit cell and PLDOS per atom of Fe 3*d*, Cu 3*d*, Cr 3*d*, and S 3*p* electron, respectively.

In Fig. 5 we have compared the measured valence-band PES spectra to the theoretical spectra, obtained from the LSDA (solid lines) and LSDA+U (dotted lines) calculations, respectively. In the LSDA+U calculations, the parameters used are $U=2.5$ eV, $J=0.94$ eV for Fe, $U=2.5$ eV, $J=0.89$ eV for Cu, and $U=1.5$ eV, $J=0.89$ eV for Cr. The theoretical spectra were obtained by adding the Fe *d*, Cu *d*, Cr *d*, and S *p* PLDOS after they are multiplied by the corresponding photoionization cross sections.[20] Only the occupied part of the weighted sum was taken for the comparison to the PES spectrum and then convoluted by a Gaussian function with 0.2 eV at full width at half maximum (FWHM) to simulate the instrumental resolution. The effects of the lifetime broadening and matrix element effects are not included in the theory curves.

The LSDA calculations show that the calculated band width is comparable to the measured valence-band width, but that the low-BE peak position does not agree with that in the measured spectrum. Such disagreement suggests the existence of the localization in FCCS, not well described in the LSDA. A possible localization mechanism in FCCS would be the large Coulomb correlation interaction between Fe, Cr, and Cu *d* electrons. Indeed, the high peak DOS near -1.0 eV shifts down by ~ 0.5 eV in the LSDA+U so that it coincides with the high spectral peak around -1.5 eV. This finding suggests the importance of the large Coulomb inter-

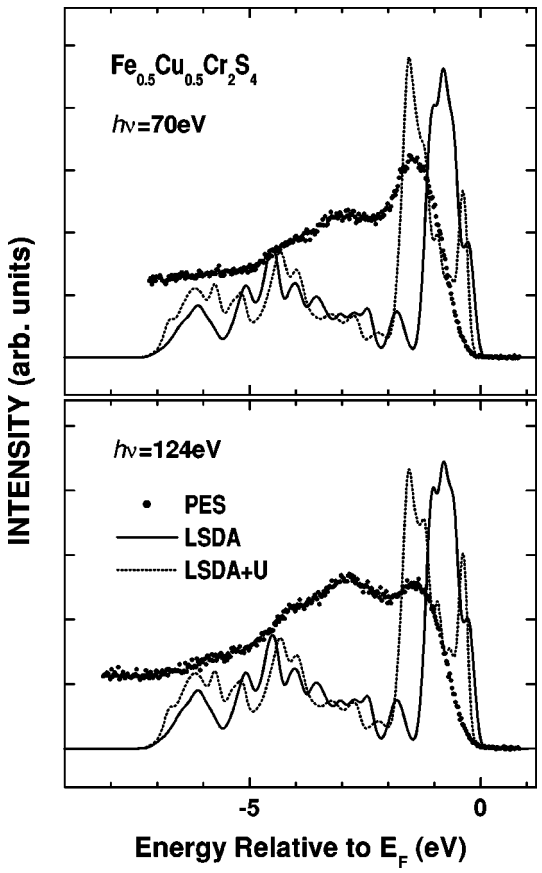

FIG. 5. Top: comparison of the $h\nu=70$ eV valence-band spectrum of FCCS (dots) to the weighted sum of the calculated PLDOSs (solid lines). Bottom: similarly for $h\nu=124$ eV. See the text for details.

actions between *d* electrons in FCCS. Nevertheless, this mechanism alone does not explain the entire discrepancy between experiment and theory. In particular, the relatively high DOS near E_F in both the LSDA and LSDA+U calculations does not agree with the low spectral intensity near E_F in the measured spectrum. This disagreement seems to reflect the smaller calculated gap size than the experimental gap size. It also suggests the existence of an extra localization in FCCS, which is not described in the LSDA or LSDA+U calculations.

Provided that the Cu ion in FCCS is monovalent, the possible valence configuration of FCCS would be $Fe_{0.5}{}^{3+}Cu_{0.5}{}^{1+}Cr_2{}^{3+}S_4{}^{2-}$ or $Fe_{0.5}{}^{2+}Cu_{0.5}{}^{1+}Cr_{1.5}{}^{3+}Cr_{0.5}{}^{4+}S_4{}^{2-}$. The former configuration has been proposed based on some experimental results.[7,26,27] This is further supported by the recent reports of the trivalency of the Cr ion by XPS (Ref. 16) and the trivalency of the Fe ion by neutron powder diffraction[28] and Mössbauer spectroscopy.[29] In this case, it is easy to understand the insulating ground state of FCCS. However, it is hard to explain the reduced magnetic moment of FCCS from that of $FeCr_2S_4$ (Ref. 30) and the wide metallic region observed in FCCS below T_C. This aspect remains to be resolved. The latter configuration is similar to that proposed by Lotgering *et al.*[7] for $CuCr_2S_4$, but is to be discarded with the trivalent Cr ion. A more precise investigation is required to determine the valence states of the Fe and Cr ions in the chalcogenide spinel compounds. An XAS study on FCCS would provide useful information because the XAS is more direct in probing the ionic valences.[31–35]

IV. CONCLUSIONS

To summarize, we have performed resonant photoemission measurements for the GMR FCCS spinel compound and compared the results to the LSDA and LSDA+U calculations. In the Cu $3p\rightarrow3d$ RPES, a negligible resonant interfence behavior has been observed for the Cu $3d$ valence band features, indicating the monovalent states of the Cu ions in FCCS. It is observed that the top of the valence-band is predominantly of the Cr $3d$ and the nearly filled Cu $3d$ electron character, whereas the Fe $3d$ electron character is rather uniformly distributed over the whole valence band, consistent with the LSDA and LSDA+U calculations. The calculated electronic structures of FCCS reveal a large hybridization of the S *p* states to the Fe and Cr *d* states, but a weak hybridization to the Cu *d* states, and predict the Fermi level to lie above the top of the complex of the Cu *d*, Fe *d*, and Cr *d* states. The LDSA+U calculation for FCCS yields better agreement with the measured valence-band PES spectra than the LDSA calculation, suggesting the importance of the large Coulomb interaction between *d* electrons. However, the low spectral intensity near E_F in the measured spectrum suggests an extra localization mechanism in FCCS.

ACKNOWLEDGMENTS

This work was supported by the KRF (Grant No. 1999-015-DP0100) and the Center for Strongly Correlated Materials Research at SNU. S.J.K. and C.S.K. acknowledge support from the KOSEF (Grant No. 97-07-02-04-01-5), and B.I.M. acknowledges support from the eSSC at POSTECH. The SRC is supported by the NSF (Grant No. DMR-95-31009).

[1] S. Jin, T. H. Tiefel, M. McCormack, R. A. Fastnacht, R. Ramesh, and L. H. Chen, Science **264**, 413 (1994).

[2] A. P. Ramirez, R. J. Cava, and J. Krajewski, Nature (London) **386**, 156 (1997).

[3] C. Zener, Phys. Rev. **82**, 403 (1951).

[4] A. J. Millis, R. Mueller, and B. I. Shraiman, Phys. Rev. Lett. **77**, 175 (1996).

[5] Z. Chen, S.T. Tan, Z. Yang, and Y. Zhang, Phys. Rev. B **59**, 11 172 (1999).

[6] J. B. Goodenough, Solid State Commun. **5**, 577 (1967); J. Phys.

Chem. Solids **30**, 261 (1969).
[7] F. K. Lotgering, R. P. van Stapele, G. H. A. M. van det Steen, and J. S. van Wieringen, J. Phys. Chem. Solids **30**, 799 (1969).
[8] J. C. Th. Holland, G. Sawatzky, and C. Haas, Solid State Commun. **15**, 747 (1974).
[9] Z. W. Lu, B. M. Klein, E. Z. Kurmaev, V. M. Cherkashenko, V. R. Galakhov, S. N. Shamin, Yu M. Yarmoshenko, V. A. Trofimova, St. Uhlenbrock, M. Neumann, T. Furubayashi, T. Hagino, and S. Nagata, Phys. Rev. B **53**, 9626 (1996).
[10] J. Matsuno, T. Mizokawa, A. Fujimori, D. A. Zatsepin, V. R. Galakhov, E. Z. Kurmaev, Y. Kato, and S. Nagata, Phys. Rev. B **55**, R15 979 (1997).
[11] G. L. W. Hart, W. E. Pickett, E. Z. Kurmaev, D. Hartmann, M. Neumann, A. Moewes, D. L. Ederer, R. Endoh, K. Taniguchi, and S. Nagata, Phys. Rev. B **61**, 4230 (2000).
[12] M.M. Ballal and C. Mande, Solid State Commun. **19**, 325 (1976).
[13] P. R. Locher, Solid State Commun. **5**, 185 (1967).
[14] C. Colominas, Phys. Rev. **153**, 558 (1967).
[15] J. Krok-Kowalski, T. Gron, J. Warczewski, T. Mydlarz, and I. Okonska-Kozlowska, J. Magn. Magn. Mater. **168**, 129 (1997).
[16] V. Tsurkan, M. Demeter, B. Schneider, D. Hartmann, and M. Neumann, Solid State Commun. **114**, 149 (2000).
[17] T. Oda, M. Shirai, N. Suzuki, and K. Motizuki, J. Phys.: Condens. Matter **7**, 4433 (1995).
[18] M. S. Park, S. K. Kwon, S. J. Youn, and B. I. Min, Phys. Rev. B **59**, 10 018 (1999).
[19] V. I. Anisimov, F. Aryasetiawan, and A. I. Liechtenstein, J. Phys.: Condens. Matter **9**, 767 (1997).
[20] J. J. Yeh and I. Lindau, At. Data Nucl. Data Tables **32**, 1 (1985).
[21] Since all the electronic states are mixed over the valence band (see Fig. 4) and the cross sections are comparable for 22 eV $\leqslant h\nu \leqslant$ 124 eV, it is difficult to separate the different local electronic states from one another.
[22] Z.-X. Shen, J. W. Allen, J. J. Yeh, J.-S. Kang, W. Ellis, W. Spicer, I. Lindau, M. B. Maple, Y. D. Dalichaouch, M. S. Torikachvili, J. Z. Sun, and T. H. Geballe, Phys. Rev. B **36**, 8414 (1987).
[23] L. C. Davis, J. Appl. Phys. **59**, R25 (1986).
[24] J.-S. Kang (unpublished).
[25] Because of the limitation in our temperature controller, we were unable to raise the sample temperature up to another metallic regims ($\simeq$340 K). The resistivity at $\simeq$340 K is higher than that at 150 K, implying a lower DOS at E_F at 340 K than at 150 K. Therefore we believe that the essential differences between the semiconducting regime and the metallic regime should be observed in the data between at 15 K and 150 K.
[26] G. Yu. Babaev, A. G. Kocharov, Kh. Ptasevich, I. I. Yamzin, M. A. Vinnik, Yu. G. Saksonov, V. A. Alferov, I. V. Gordeev, and Yu. D. Tret'yakov, Kristallografiya **20**, 550 (1957) [Sov. Phys. Crystallogr. **20-3**, 336 (1975)].
[27] E. Riedel, R. Karl, and R. Rackwitz, J. Solid State Chem. **40**, 255 (1981).
[28] H. M. Palmer and C. Greaves, J. Mater. Chem. **9**, 637 (1999).
[29] H. N. Ok, K. S. Baek, H. S. Lee, and C. S. Kim, Phys. Rev. B **41**, 62 (1990).
[30] H. M. Palmer and C. Greaves, Physica B **276-278**, 568 (2000).
[31] G. Subias, J. Garcia, M. G. Proietti, and J. Blasco, Phys. Rev. B **56**, 8183 (1997).
[32] J.-H. Park, T. Kimura, and Y. Tokura, Phys. Rev. B **58**, R13 330 (1998).
[33] B. Ammundsen, D. J. Jones, J. Roziere, and G. R. Burns, Chem. Mater. **8**, 2799 (1996).
[34] N. Treuil, C. Labrugere, M. Menetrier, J. Portier, G. Campet, A. Deshayes, J.-C. Frison, S. J. Hwang, S. W. Song, and J. H. Choi, J. Phys. Chem. B **103**, 2100 (1999).
[35] C. Branci, J. Sarradin, J. Olivier-Fourcade, and J. C. Jumas, Chem. Mater. **11**, 2846 (1999).